PROF. HENG-MU ZHANG (Orcid ID : 0000-0002-3144-585X)

DR RUI XIA (Orcid ID : 0000-0003-2409-1181)

DR AIMIN WU (Orcid ID : 0000-0001-8322-8833)

MicroRNAs play important roles in regulating rapid growth of the *Phyllostachys edulis* culm internode

Kai-li Wang[1, 2], Yuanyuan Zhang[1, 2] (0000-0001-7657-1625), Heng-Mu Zhang[3] (0000-0002-31244-585X), Xin-Chun Lin[4] (0000-0003-0168-331X), Rui Xia[1,5] (0000-0003-2409-1181), Lili Song[4*], Ai-Min Wu[1, 2,5*] (0000-0001-8322-8833)

[1] The State Key Laboratory for Conservation and Utilization of Subtropical Agro-bioresources, South China Agricultural University, Guangzhou, 510642, China

[2] Guangdong Key Laboratory for Innovative Development and Utilization of Forest Plant Germplasm, College of Forestry and Landscape Architectures, South China Agricultural University. Guangzhou, 510642, China

[3] Institute of Virology and Biotechnology, Zhejiang Academy of Agricultural Sciences, Hangzhou 310021, China

[4] The State Key Laboratory of Subtropical Silviculture, School of Forestry and Biotechnology, Zhejiang A&F University, Lin'an, 311300, China;

[5] Guangdong Laboratory of Lingnan Modern Agriculture, Guangzhou 510642, China

* Corresponding author: wuaimin@scau.edu.cn (AM. Wu) and lilisong@zafu.edu.cn (L. Song)

This article has been accepted for publication and undergone full peer review but has not been through the copyediting, typesetting, pagination and proofreading process, which may lead to differences between this version and the Version of Record. Please cite this article as doi: 10.1111/NPH.17542

Received: *4 February 2021*

Accepted: *29 May 2021*

Summary

- Moso bamboo (*Phyllostachys edulis*) is a fast-growing species with uneven growth and lignification from lower to upper segments within one internode. MicroRNAs (miRNAs) play a vital role in post-transcriptional regulation in plants. However, how miRNAs regulate fast growth in bamboo internodes is poorly understood.
- In this study, one moso bamboo internode during early rapid growth was divided into four segments regarded as F4 (bottom) to F1 (upper) and then were analyzed by transcriptomes, miRNAs and degradomes.
- The F4 segment possessed a higher number of actively dividing cells as well as a higher content of auxin (IAA), cytokinin (CK) and gibberellin (GA) comparing with F1 segment. RNA-seq analysis showed DNA replication and cell division associated genes highly expressed in F4 rather than that in F1. A total of 63 differentially expressed miRNAs (DEMs) were identified between F4 and F1. Degradome and transcriptome implied many downstream transcription factors and hormonal responses genes were modulated by DEMs. Several miR-targets interactions were further validated via tobacco co-infiltration.
- Our findings provide new insights into miRNA-mediated regulatory pathways in bamboo, which will contribute to a comprehensive understanding of the molecular mechanisms governing rapid growth.

Keywords: *Phyllostachys edulis*, internode, rapid growth, hormone, microRNA, degradome

Introduction

Plant development consists of many stages starting from cell division to elongation, maturation and lignification. There are slight and smooth transition procedures between these stages. Studies on such transition from primary to secondary growth are of particular interest for understanding mechanisms of rapid plant growth regulation, especially in forest trees. Populous, Bamboo and Eucalyptus can grow very fast in suitable conditions and are regarded as model systems to study the mechanisms underlying rapid growth. Rapid growth in plants is affected by several factors including degree of cell proliferation, cell elongation, hormonal responses, and other related factors. Plant size is determined by cell number and size, which are related to cell proliferation and cell elongation (Bundy *et al.*, 2012).

Cell division and growth defects in *Pseudosasa japonica* var. *tsutsumiana* resulted in slow growth (Wei *et al.*, 2018). The plant primary cell wall (PCW) has a major role in cell expansion and elongation, as cells increase in size by selective turgor changes in the PCW (Cosgrove, 2015; Kumar *et al.*, 2016; Loix *et al.*, 2017). Furthermore, cell wall composition and arrangement of cell wall components also alters with elongating plant cells (Irshad *et al.*, 2008). Cell proliferation and elongation is also modulated by different plant hormones (Wang *et al.*, 2015). Enhanced extensibility in the cell wall needs upregulation of auxin and cytokinin (CK) (Tameshige *et al.*, 2015). Plant endogenous hormones including auxin, CK, gibberellin (GA), abscisic acid (ABA) and ethylene affect physiological processes at very low concentrations (Davies, 2010). The activities of auxin and GA is overlapping in cell expansion (Weiss & Ori, 2007). Auxin is involved in many developmental processes such as apical dominance, organ formation and gravitropism in different concentrations. The active auxin that are most well-studied is indoleacetic acid (IAA) (Korasick *et al.*, 2013; W. Wang *et al.*, 2017; Nanda & Melnyk, 2018). GAs are diterpenoids with the primary function of promoting cell expansion, differentiation and proliferation (Eriksson *et al.*, 2006; Yamaguchi, 2008; Daviere & Achard, 2013; Claeys *et al.*, 2014). CKs participate in many plant developmental processes including cell division, lateral root formation and meristem maintenance, organ size regulation, developmental transitions, and regulation of leaf senescence. CKs can also respond to stresses through interactions with auxin

(Schaller *et al.*, 2015; Nanda & Melnyk, 2018; Cortleven *et al.*, 2019). Auxin and CK can regulate tiller number which contributes to the special structure of rice (Wen *et al.*, 2020). ABA is a growth inhibitor that presents in vascular plants and mosses, and also functions as an essential regulator of many plant processes such as dormancy, seed development, germination and responses to abiotic stress (Liu *et al.*, 2003; Olds *et al.*, 2018; Takatsuka & Umeda, 2019).

Plant hormones crosstalk with each other to regulate plant growth and development. For example, CKs interact antagonistically with auxin and negatively regulate xylogenesis, GAs promote auxin transport by modulating PINs while auxin triggers GA biosynthesis or accumulation (Nanda & Melnyk, 2018). ABA can inhibit root cell elongation through repressing cytokinin signaling (Takatsuka & Umeda, 2019). Cells achieve their final size and shape after development of secondary cell walls and initiate lignification after cell differentiation (Rogers & Campbell, 2004; Wang *et al.*, 2013). Appropriate level of lignin deposition is necessary for plant development (Yoon *et al.*, 2015) as any decrease in lignin content can cause dwarfism in plants. On the contrary, higher lignin content can give more strength to plants and their cell wall components (Muro-Villanueva *et al.*, 2019).

MicroRNAs (miRNAs) are endogenous, non-coding small RNAs approximately 22 nt in length. Mature miRNAs can negatively regulate their target genes by inhibiting or degrading the transcripts (Rooij & Olson, 2007). Degradome sequencing is an important approach to further predict degradation of target genes by miRNAs (Kuang *et al.*, 2019). Many miRNAs participate in plant growth. In the rapid growth stage of moso bamboo (*Phyllostachys edulis*), many miRNAs and their target genes participate in rapid growth of the culm and modulate multiple biological processes. Some miRNAs related to meristem and morphological development are also involved in synthesis of many endogenous hormones like GA, CK and auxin in bamboo shoot (Jin *et al.*, 2016). MiRNAs coevolve with their target genes (Zhao *et al.*, 2014). MiR397 can regulate lignin content via modulating a laccase involved in lignin biosynthesis in *Arabidopsis* (Wang *et al.*, 2014). MiR396 regulates the protein level of *GROWTH-REGULATING FACTOR*s (*GRF*s) and affects cell proliferation in the meristem as well as in developing leaves (Mecchia *et al.*, 2013). MiR164 targets *PeNAC*s which may play important roles in secondary cell wall (SCW)

biosynthesis and lignification in bamboo shoots (Shan *et al.*, 2019). Previous research suggested that highly conserved miRNAs may play more essential roles in the earlier developmental stage of moso bamboo due to stress responses (He *et al.*, 2013). The ratio of highly conserved miRNAs families in moso bamboo (Monopodial Bamboo) is lower than that in ma bamboo (Sympodial Bamboo) while the proportion of less conserved miRNAs is higher. The high proportion of less conserved miRNAs in moso bamboo results in better adaptation to environmental fluctuations than ma bamboo (Zhao *et al.*, 2014).

Moso bamboo (*P. edulis*) belongs to monophyletic BEP clade (Bambusoideae, Ehrhartoideae, Pooideae) of the grass family (Poaceae) (Li *et al.*, 2016). Bamboo is one of the fastest growing lignocellulose-abundant plants and is an important non-timber forest resource globally (Zhou *et al.*, 2005; Peng *et al.*, 2010). During its peak growing season in spring its shoots can grow up to 1 m in length per day and then reach a maximum height of about 20 m within 45 to 60 days (Peng *et al.*, 2010; Peng *et al.*, 2013a). The growth of bamboo culm has distinct characteristics among different segments, the bottom internode is older than the upper one and lignin content in the bottom internode is higher than that in the upper portion while it is opposite within internodes (Tsuyama *et al.*, 2017; Wang *et al.*, 2019). Elongation of bamboo internodes is influenced by cell division and elongation. Bamboo culms undergo rapid cell division during their early stages of growth. Later, it is overtaken by cell elongation and lignification (He *et al.*, 2013; Wang *et al.*, 2015). Cell wall metabolism and lignin biosynthesis related genes are largely expressed in the basal portion of the culm, whereas cell formation and DNA synthesis-related genes involved in meristem maintenance are highly expressed in the upper portion of the culm (Gamuyao *et al.*, 2017). Almost all genes related to cell wall metabolism and cell morphogenesis including *Expansin* (*EXP*), *Cellulose synthase A* (*CesA*), *Cellulose synthase-like* (*CSL*) and lignin biosynthesis genes were highly up-regulated during bamboo culm development (Peng *et al.*, 2013b).

The elongation of bamboo culm is due to internode expansion, but details related to the biology of individual bamboo internodes is poorly understood. In this study we measured the variation in miRNAs and their target genes as well as the associated hormone distribution at different

segments within one internode during rapid growth in moso bamboo. We revealed that the accumulation of downstream target transcripts coordinately varied with upstream miRNA levels. These target genes were mainly characterized as *GRF*s, *Auxin response factor*s (*ARF*s) and others involved in hormone biosynthesis, all of which affected cell growth.

Materials and Methods

Plant material collection

Approximately 1.6 ~ 1.7 m bamboo culms were harvested in April 2018 from YuHang District of Zhejiang province, China. The growth rate of bamboo culm was measured at 1.6 ~ 1.7 m height after every 2 hours daily (Fig. S1a). Samples were collected during maximum growth rate stage of culm at 22:00 (Fig. S1a). Internodal lengths were measured every 24 hours by labelling and pealing the sheath. Finally, we measured 15 culms at each time point for 6 days (Fig. S1b, c). We labeled the longest internode at 0 day as I(0), above internodes labeled as I(1), I(2), I(3) … and below internodes labeled as I(-1), I(-2), I(-3) …. (Fig. S1b). The target internode (7 ~ 8 cm) above the longest internode was cut into four equal-length sections and labeled F1-F4, corresponding to upper parts, upper-middle, lower-middle and internode bottom basing on method of Brown *et al*., (2005). The 1/4 bottom part of internode above collected internode was also harvested and named UF4 (Fig. S2). The samples were immediately dipped in liquid nitrogen and stored at -80°C for RNA extraction. All samples were collected in three biological replications and later were used for transcriptome analysis.

Microscopic observation

The 0.5 cm^3 fresh samples were fixed into formalin-acetic-50% alcohol (FAA, v/v) solution. Paraffin sections (20 μm) under light microscope were observed after being stained in safranin O and fast green FCF solutions. After staining, the samples were fixed using 2.5% glutaraldehyde fixative solution and 2 μm sections were observed under transmission electron microscope.

Hormone content determination

Approximately 2 g F1 and F4 samples with three biological replications were sent to Greensword Creation Technology Company (Wuhan, China). The content of endogenous indoleacetic acid

(IAA), abscisic acid (ABA), gibberellic acids (GA1, 3, 4 and 7) and cytokinins (CKs, iP, isopentenyladenine; tZ, trans-zeatin; cZ, cis-zeatin and DZ, dihydrozeatin) were determined by previously published methods (Liu *et al.*, 2010; Chen *et al.*, 2012) with slight modifications.

RNA extraction

Transcriptome RNA library construction and RNA sequencing were done from fifteen samples (F1-F4 and UF4) using RNAprep Pure Plant Kit (Polysaccharides & Polyphenolics-rich, TIANGEN) following manufacturer's instructions. The sRNA construction and total RNAs sequencing was done from six samples (F1 and F4) using Trizol method (93289, Sigma). Samples F1 and F4 were used for degradome library construction and sequencing. The quality and nucleic acid concentration in all RNAs samples were accessed using agarose gel electrophoresis (1%, Tanon 3500R), Nano Drop®ND-1000 UV Spectrophotometer and RIN (RNA Integrity Number, Nanodrop GX), respectively.

RNA library construction and sequencing

Fifteen RNAs which passed the quality test were analyzed by Biomarker Technology Co. (Beijing, China, https://www.biocloud.net/) on an Illumina instrument. A total 1 μg RNA per sample was used as input material for the RNA sample preparations. Sequencing libraries were generated using NEBNext UltraTM RNA Library Prep Kit for Illumina (NEB, USA) following manufacturer's recommendations. Firstly, mRNA was purified from total RNA using poly-T oligo-attached magnetic beads. Then the first and second strand cDNA was synthesized. Remaining overhangs were converted into blunt ends via exonuclease / polymerase activities. NEBNext Adaptor with hairpin loop structure was ligated to DNA fragments which after adenylation of 3' ends prepare for hybridization. The library fragments were purified with AMPure XP system (Beckman Coulter, Beverly, USA). Then 3 μL USER Enzyme (NEB, USA) was used with size selected, adaptor-ligated cDNA at 37°C for 15 min followed by 5 min at 95°C before PCR. Then PCR was performed with Phusion High-Fidelity DNA polymerase, universal PCR primers and Index Primer. At last, PCR products were purified (AMPure XP system) and library quality was assessed on the Agilent Bioanalyzer 2100 system. The clustering of the index-coded samples was performed on a cBot Cluster Generation System using TruSeq PE Cluster Kit

v4-cBot-HS (Illumia) according to the manufacturer's instructions. After cluster generation, the libraries were sequenced on an Illumina platform and paired-end reads were generated. After quality control, the adaptor sequences and low-quality sequence reads were removed from the data sets. Raw sequences were transformed into clean reads after data processing. These clean reads were then mapped to the reference genome sequence. Hisat2 tools software was used to map with reference genome. Gene function was annotated based on databases including NR (NCBI non-redundant protein sequences); NT (NCBI non-redundant nucleotide sequences); Pfam (Protein family); KOG/COG (Clusters of Orthologous Groups of proteins); Swiss-Prot (A manually annotated and reviewed protein sequence database); KO (KEGG Ortholog database); GO (Gene Ontology). And the differentially expressed genes (DEGs) were observed by BMKCloud with DESeq2_EBSeq software and parameters were false discovery rate (FDR) ≤ 0.05 and $|\log_2 FC|$ (FC, fold change) ≥ 1.

Small RNA and degradome sequencing and target genes prediction

Sample F1 and F4 with three replications were used to analyze miRNAs. After the samples passed the quality control, library for sRNA sequencing was developed. First, the 3' SR and 5' SR adaptors were ligated, followed by reverse transcription synthesizing first chain. Finally, after PCR amplification and size selection, the PCR products were purified (AMPure XP system) and library quality was assessed after screening fragment. After cluster generation, the library preparations were sequenced on an Illumina platform and single-end reads were generated. Raw sequences were transformed into clean reads after quality control step. Using Bowtie tools software, the clean reads were aligned with Silva, GtRNAdb, Rfam and Repbase databases, respectively, and the abundance of each type RNAs was counted. The remaining reads were detected as known miRNA or novel miRNA predicted by comparing with genome and known miRNAs from miRBase. Randfold tools software was used for novel miRNA secondary structure prediction. To determine the target genes, the miRNA sequences of F1 and F4 were blasted to miRBase and joined to the transcriptome. And the differentially expressed miRNAs (DEMs) were observed by BMKCloud with DESeq2_EBSeq software and parameters were FDR ≤ 0.05 and FC ≥ 1.5.

Degradome sequencing libraries about F1 and F4 were generated after samples passed the quality test. cDNA was synthesized by mixed reverse transcription of Biotinylated Random Primers after mRNA was caught by magnetic bead and ligated 5′ adaptor. The library preparations were sequenced on an Illumina platform after PCR. Following quality control, clean tags and cluster tags were obtained and mapped to the reference genome sequence. The cluster tags were compared with the Rfam database, the ncRNAs obtained by sequencing were classified. The remaining reads were used to detect the cleavage sites of target genes. The cleavage sites of target genes were determined by Cleaveland software with *p*-value $\leqslant$ 0.05 and Target plots (t-plots) (Addo-Quaye *et al*., 2008; German *et al*., 2008). The target genes annotation information was obtained through sequence mapping to NR, Swiss-Prot, GO, KEGG, KOG/COG, KEGG databases. All RNA_seq, miRNA and degradome datasets were submitted to http://bigd.big.ac.cn/gsa/ with submission number CRA003878.

qPCR analysis and gene verification

RNAs of fifteen samples that were used for transcriptome sequencing were also used for qPCR (quantitative real time PCR). The cDNA synthesis used PrimeScript™ RT Master Mix following manufacturer's instructions (RR036A, TaKaRa). Randomly selected genes were analyzed and verified by qPCR, the gene-specific primers were shown in Table S1. *NTB* was used as the internal control (Fan *et al.*, 2013). The PCR protocol was 95°C 30s, 95°C 5s, 60°C 30s for 40 cycle analyzed by LC480 (Roche). The relative abundance of each gene was calculated from the $2^{-\Delta Ct}$ referenced to *NTB*, with three replicates for each reaction. The miRNA qPCR special method was based on a previously published method and U6 was chosen as the control for small RNAs (Ge *et al.*, 2017). MiR_N17, miR_N31, miR396a-3, miR444b-1 and their target genes including *PH02Gene29128*, *PH02Gene45537*, *PH02Gene01484* and *PH02Gene21974* were selected to verify the interaction between miRNA and target gene. The interaction verification method of miRNA and target genes was referenced to Long *et al* (2016) with slight modification, primers were shown in Table S1. The sequences of target genes were 150 ~ 220 bp including the target sites were inserted into pEarlyGate103 vectors (Earley *et al*., 2006) to form the target genes fused with GFP protein. Then the vectors with miRNA and target genes were transferred into

agrobacteria, respectively, and finally injected into tobacco leaves. The tobacco leaves were observed under Nightshade LB 985.

Results

Cell morphology varies within the internode of bamboo culms

In order to study the mechanism of cell growth in bamboo, an individual internode of the bamboo culm was analyzed. To decide which internode has high growth potential, we measured length of nine internodes in the following 2 days, and found that the second I(2) and third I(3) internodes of above longest internode grow fastest, so in this study we chose I(3) as target internode to analyze (Fig. S1b, c). The target internode was divided into four segments referred as F1-F4 (Fig. 1), and the base segments of the upper internode were regarded as UF4 (Fig. 1; S2). There was an increasing trend in cell size from F4 to F1 segments. The cell number gradually decreased from F4 to F1 whereas cell length increased (Fig. 1m-n). The F4 sample had smallest and tightly packed cells whereas F1 cells were larger in size and loosely arranged (Fig. 1a-d). Cell wall thickening gradually increased from F4 to F1. F1 exhibited the thickest wall whereas F4 was the thinnest across all samples (Fig. 1e-h). Additionally, there were different division cells in F4 segment, but without division cells in F1 (Fig. 1i-l). Results indicated that the cells conditions from F4 to F1 segments showed the trends from tender to mature within the individual internode.

Hormone distribution in the internode

Content and distribution of hormones closely relate to plant growth. To determine whether hormonal distribution was related to morphological differences within one internode of bamboo, GAs, CKs, auxin and ABA were detected in F1 and F4. F4 had a higher content of auxin (IAA), four types of active GAs (GA1, 3, 4, 7) and two types of active CKs (iP and CZ, while cZ and DZ of CKs were not detected) than those in F1. ABA content, in contrast, was higher in F1 than that in F4 (Fig. 2). Hormonal distribution was consistent with cell morphology as more young and dividing cells were present in F4 and more mature cells with larger size and thicker cell wall in F1.

Transcriptome analysis reveals genetic difference in internode

To clearly explain cell growth and morphological differences among each segment, the transcriptome was analyzed. Transcriptome of all biological replicates in each segment (F1-UF4) highly correlated ($r^2 > 0.9$) (Fig. S3), indicating a high degree of repeatability among samples, thus confirming that the results were appropriate for further analysis. Summary of transcript reads mapping was shown in Table S2.

Twenty gene profiles clustered together based on their expression patterns (Fig. S4a). In cluster 8 with 7414 genes, gene expression levels decreased from F4, 3 to F2, 1 then rose again in UF4. Gene expression level of cluster 18 and 9, with 3180 and 2885 genes, respectively, roughly increased from F4, 3 to F2, 1 whereas decreased in UF4, opposite to cluster 8. By KEGG pathway annotation, most genes in cluster 8 were associated with genetic information processing such as translation and transcription, which are related to cell division. Cluster 9 and 18 exhibited similar KEGG pathway annotation. Most genes associated with metabolism such as carbohydrate metabolism and biosynthesis of other secondary metabolites (Fig. S4b-d).

Then all F1, F2, F3 and UF4 were compared with F4 using FDR ≤ 0.05 and $|\log_2 FC| \geq 1$ as threshold, the DEGs number increased from F3 VS F4 (295) to F1 VS F4 (10236) while the DEGs number in UF4 VS F4 (528) was lower than that of F2 VS F4 (3685) but higher than that of F3 VS F4. Down-regulated DEGs were lower than up-regulated DEGs in each compared group except for F3 VS F4 (Fig. S5). In Fig. S5, DEGs of F2 VS F4 and F1 VS F4 were higher in total count than DEGs in F3 VS F4 and UF4 VS F4.

Up-regulated UF4 VS F4 DEGs concentrated on pathways related to cell growth including plant hormone signal transduction, starch and sucrose metabolism, amino and nucleotide sugar metabolism, and zeatin biosynthesis (Fig. S6d, h). There were only a limited number of down-regulated DEGs, most of which were involved in photosynthesis.

KEGG pathway enrichments of the DEGs were acquired from RNA transcriptomes of F1-F3 compared to that of F4, respectively (Fig. S6). More and more up-regulated DEGs in the three analyzed groups enriched in phenylpropanoid biosynthesis from F3 VS F4 to F1 VS F4 (Fig. S6a-c). Down-regulated DEGs gradually increased from F3 VS F4 to F1 VS F4 and mainly associated with DNA replication, which are related to cell division (Fig. S6e-g). The expressions

of six randomly selected cell division associated genes (*PH02Gene05832*, *PH02Gene14407*, *PH02Gene21199*, *PH02Gene29871*, *PH02Gene32591* and *PH02Gene45202* (Table S1) were verified with qPCR and regular changes (Fig. S7). In general, their expression levels in F4 were clearly higher than that in F1, and in UF4 the expression was high again. The expressions were consistent with the transcriptome data.

MiRNA and degradome analysis reveal inner relationship with target genes

MiRNAs negatively regulate their target genes by inhibiting or degrading their transcripts. To examine whether certain parts of transcriptome changes were related to miRNA regulation in bamboo internodes, miRNA and degradome library of F1 and F4 were conducted. In total, 740 miRNAs (664 known and 76 novel miRNAs) and 63 DEMs (51 known and 12 novel miRNAs, 13 down-regulated and 50 up-regulated) of 734 target DEGs (F1 compared with F4, FDR $\leq$ 0.05) were identified in two samples (Fig. 3; Fig. S8). In fact, the up-down miR-target expressed pattern (miRNA up-regulated and corresponding target gene down-regulated) had 426 pairs and down-up pattern had 70 pairs. The most abundant miRNA of known DEMs was miR396, and the second was miR167. Expression levels of novel DEMs were generally lower than known ones (Fig. 3).

The 734 DEGs were grouped into 11 clusters using STEM software based on their expression patterns (Fig. S9). Significantly different clusters 8, 9, 18 and another cluster 16 were selected for KOG analysis (Fig. 3) and related KEGG pathways were investigated (Fig. S10). Cluster 8 had the most DEGs (304), and 252 genes belonged to the up-down miR-target expressed pattern. The gene expression trend roughly decreased from F4 and F3 to F2 and F1 then rose again in UF4. Interestingly, there were many cell division genes in the cluster 8 KOG distribution. The second abundant group was cluster 9 with 112 genes that showed roughly opposite gene expression trends with cluster 8. There were 17 genes belong to down-up miR-target expressed pattern in cluster 9. The number of genes related with cell division were decreased and among them many genes were related to other transport and metabolism process including protein, carbohydrate, inorganic ion and secondary metabolites. The third abundant group was cluster 18 with 143 genes with expression trends increased from F4 to F2 and F1 then decreased again in UF4, and there were 23 genes belong to down-up miR-target expressed pattern in cluster 18. KOG distribution of cluster

18 was similar to cluster 9 where genes were more related to other transport and metabolism process such as lipid, secondary metabolites, carbohydrate, amino acid and so on.

The degradomes of F1 and F4 were further analyzed (Table S3). Total 131 miRNA target genes, including 21 DEGs which were regulated by 12 DEMs, were degraded in F1 and F4 samples (Fig. 4; Table S4). In total there were 66 miR-target pair genes including 54 pairs of up-down pattern and 3 pairs of down-up pattern. These 21 genes were divided into two groups based on their expression patterns (Fig. 5). In general, gene expression gradually decreased from F4 to F1 and increased in UF4, and was grouped in Class I. The expressed trend on the contrary was grouped in Class II. The annotation of these 21 genes was associated with growth regulating factors (GRFs), auxin response factors (ARFs) and NAC domain factors. There was one *ARF6* and two *ARF8* targeted by miR167 and eleven *GRF*s (*1*, *4*, *5*, *6*, *7*, *8*, *9*, *10*) targeted by miR396 (Table S4) in F1 and F4 degradomes.

Gene verification of transcriptome and miRNA

In order to validate reliability of the transcriptome and degradome, genes related with cell cycle, auxin, ABA, carbohydrate metabolic, etc. were selected for qPCR analysis (Table S1; Fig. 5a-l). The expression levels of genes related to cell cycle, division and auxin decreased gradually from F4 to F1 and then rose again in UF4 (Fig. 5a-c, g, i-l). The expression level of genes related with secondary cell wall and ABA approximately increased from F4 to F1 then decreased in UF4 (Fig. 5d-f, h). Expression profiles of these genes were consistent with RNA-seq data.

Further, six DEMs PemiR164a-3, PemiR167d-4, PemiR396e-4, PemiR396f-3, PemiR529d, PemiR529e-2 and their nine target genes were selected for expression level analysis (Table S1; S5; S6; Fig. 5m-u). In Fig. 6 the expression level of PemiR164a-3, PemiR167d-4, PemiR396e-4 and PemiR396f-3 roughly increased from F4 to F1. The expression levels of their target genes *PH02Gene39446*, *PH02Gene37247*, *PH02Gene34199*, *PH02Gene23920*, *PH02Gene43240*, *PH02Gene08777* and *PH02Gene01484* were roughly decreased from F4 to F1 (Fig. 5m-s). Whereas expression levels of PemiR529d, PemiR529e-2 and their target genes *PH02Gene07908* and *PH02Gene09964* showed the opposite pattern (Fig. 5t, u). This indicated that expression profiles of miRNAs and their target genes were complementary.

Some miRNA cleavage sites were predicted by Target plots shown in Fig. S11. To further examine whether our novel miRNA can indeed inhibit the target genes, miR_N17, miR_N31, miR396a-3 and miR444b-1 were tested (Fig. 6). All 21 nt except miR_N17 (22 nt) were up-regulated from F4 to F1, however, miR444b-1 was down-regulated. The *PH02Gene29128* (*SKP2A*), *PH02Gene45537* (phosphatase), *PH02Gene01484* (*GRF10*) and *PH02Gene21974* (*MADS27*) were miR_N17, miR_N31, miR396a-3 and miR444b-1 candidate target genes, respectively, their expression pattern was opposite to the expression pattern of miRNAs. Furthermore, miR396a-3 and miR444b-1 can cleave target genes *PH02Gene01484* and *PH02Gene21974*, respectively, in degradome (Fig. S11). MiR_N17 and miR_N31 inhibit expression of *PH02Gene29128* and *PH02Gene45537* target genes, respectively. The target genes fused with GFP protein. After co-overexpression of every pair vector (Table S1; Fig. 6a) into tobacco leaf, GFP fluorescence clearly decreased as compared to co-infiltrated leaves of target genes and empty vector (Fig. 6c, d), suggesting that miR_N17, miR_N31, miR396a-3 and miR444b-1 indeed acted on their target sites and negatively regulated their expression.

MiRNA, targets and hormone network in bamboo internode

In order to better exhibit the underlying relationship of miRNAs, target genes, hormones and cell growth process, based on our data and previous reports (Hake *et al.*, 2004; Shinozaki & Yamaguchi-Shinozaki, 2006; Perrot-Rechenmann, 2010; Inagaki & Umeda, 2011; Schaller *et al.*, 2015; Yu *et al.*, 2020), we created a hypothetical network that regulates bamboo internode rapid growth (Fig. 7).

There were twelve families of miRNAs including four novel family's miRNA participating in internode growth (Fig. 7). All miRNAs negatively regulated their target genes. These genes promoted, participated or inhibited downstream genes and were linked to hormonal pathways, their final destination was to regulate cell division, cell elongation and cell wall thickness processes.

MiRNAs can be divided into two groups based on their target genes. MiR_N47, miR164, miR396, miR528, miR_N64 and miR167 mainly acted on the bottom internode segment F4 at lower

expression level and mainly participated in cell division, while miR529, miR396a, miR164a, miR_N39, miR2275, miR444, miR397 and miR_N21 acted on internode upper segment F1 related with cell elongation and cell wall thickness (Fig. 7). In fact, the target types of miR396 were most abundant including *RECA*, *GRF*s, cyclin, and xyloglucan related genes.

In this network, many miRNAs target the same type of genes for example miR396 and miR164 both targeted *RECA* or their target genes are involved in the same processes, such as *GRF1*, target of miR396, and *GA2OX1*, target of miR_N64, both participate in the GA signaling pathway.

Discussion

P. edulis (Bamboo) is one of the most fast-growing lignocellulose-abundant plants, in fact its shooting speed can reach 1 m/d in spring (Peng *et al.*, 2010). Thus, bamboo is an excellent model for studying the mechanisms of plant rapid growth. Bamboo culms fast-growth is attributed by cell division and the cell elongation, especially contributed by each internode. During early stages, the internode is short and most cells have a strong ability to divide or elongate. During growth, differences in cells appear between the bottom and upper segments of the internode. The cells transition from the actively dividing phase at the bottom segment to the cell elongation phase at the upper segment, with the cell wall gradually thickening. Cells in the bottom segments of the internode maintain relatively strong cell division ability (Suzuki & Itoh, 2001). In our results, cell morphology in F4-F1 was the epitome of growth including cell size, number and cell wall thickness. Since the cells in the bottom segment of the internode (F4) have a high division potential, they are small and tightly packed and arranged. However, cells in the upper segment of the internode (F1) were more mature and longer, which is consistent with previous studies. The cells change from dividing phase to elongating phase and cell wall thickness in each internode suggests that the bamboo internode is an excellent system for studying fast-growth mechanisms.

Higher cell growth relative hormones at the bottom compared to upper internode segments resulted in higher cell division

In whole moso bamboo culm, during rapid growth stage, the hormonal distribution was uneven. In growing culm, auxins, CKs and GAs were present at the shoot apex, while ABA mainly

accumulated on the lower part of the culm (Gamuyao *et al*., 2017). However, in one internode, we found that auxin, GAs and CKs were higher in the bottom segment (F4), while ABA was higher at the upper segment (F1), which were consistent with findings with Gramineae (Fan *et al.*, 2017).

The relationship between the rapid growth of moso bamboo and hormones is inseparable. Function of auxin is more complicated and diverse in moso bamboo, since there are more auxin related genes in bamboo than in *Arabidopsis* and rice (W. Wang *et al.*, 2017). Exogenous application of GA resulted in a significant increase in internode length (Zhang *et al.*, 2018). Cell elongation (maturation) and cell division exhibit negative correlation during bamboo culm growth. When cell size increases their ability of division reduces or vice versa (Wang *et al.*, 2015). Many genes related to plant hormones including auxin, brassinosteroid (BR), GA and CK were up-regulated in bamboo culm during development (Peng *et al.*, 2013b). Based on Fig. S5; 6, internode bottom was younger than the upper portion and hormones were distributed unevenly. The results were consistent with Gamuyao *et al* (2017). Tao *et al* (2020) also found in whole bamboo culm the IAA content gradually decreased in the order of SD (starting of cell division) > RD (Rapid division) > RE (Rapid elongation), this phenomenon was benefit to cell elongation. Thus, it is proposed that rapid growth in bamboo culm may be due to interplay of various hormones with auxin being the main contributor.

Additionally, UF4 VS F4 DEGs were partly enriched in specific KEGG pathways (Fig. S6). Among up-regulated DEGs of UF4 VS F4, zeatin biosynthesis is well-marked and zeatin belongs to CKs (Jaworek *et al.*, 2019). Thus, the bamboo cell division might be tightly related to CKs.

Cell division ability in the internode from bottom to the top gets weaker

Clusters of total genes and KEGG pathway annotation of cluster 8, 9 and 18 (Fig. S4) showed that during internode growth, cell division related gene expression levels roughly decreased from base (F4) to upper (F1) and increased again in UF4 which was the next internode bottom segment, but the metabolism related genes expression level was on the opposite. DEGs number also varied considerably between F4, F3, F2 VS F1 (Table S1). As the upper internode got more mature the

cell's division ability got weaker. The cell division ability gradually reduced from F4 to F1 (Fig. 1). Meanwhile, phenylpropanoid biosynthesis was enriched in up-regulated DEGs (Fig. S6). Phenylpropanoid pathway is important for lignin biosynthesis (Vanholme *et al.*, 2019). Compared with tender tissues, more expressed genes associated with phenylpropanoid in mature parts of moso bamboo have been reported (Gamuyao *et al.*, 2017). The F3 and F4 segments were tender and mainly processed in cell division while F1 and F2 were older and were undergoing the cell elongation, thickness and lignin accumulation (Fig. 1). In bamboo culm the lignin content increased with maturity thus young culms under active proliferation, expansion and differentiation produced less lignin. NAC factors are master regulators for secondary cell wall thickening (Wang *et al.*, 2011). NAC domain factors show an upward trend from F4 to F1 which corresponds to an increase in lignin content (Fig. 4). This is most likely why F1 cell wall thickness is greater than F4 cell wall thickness (Fig. 1). These results are consistent with Tao *et al* (2020) study of whole bamboo culms, where they found high levels of lignin and cellulose in the RE phase. Different from our studies within individual internode, they fetched three types internodes from different height. It is also consistent with our results that most DEGs among three type internodes were mainly related to cell division, cell cycle, cellulose, lignin synthesis and plant hormone pathway. Meanwhile genes involved in cell cycle and division were mostly expressed in SD (Tao *et al.*, 2020). Our results are also consistent with the report of Wei *et al* (2019), who divided one internode of *Bambusa multiplex (Lour.) Raeusch. ex Schult.* from bottom to top into three parts: division zone, elongation zone and elongation completion zone. The DEGs between fastest growth internode and the growth decreasing internode were consisted to cell division, cell cycle and other pathways (Wei *et al.*, 2019). Although all these studies showed similar results that cell division related genes were highly expressed in bottom segments while elongation and lignification genes preferentially expressed in upper segments. However, present study was more focused on miRNA and DEMs regulated target genes to explain why the DEGs from bottom to upper segments show these changes.

MiRNAs and their targets co-regulated the cell growth process

MiRNAs negatively regulate their complementary mRNAs at a posttranscriptional level (Kurihara & Watanabe, 2004). In our results, the expressed level of most novel DEMs was low (Fig. 3), which was consistent with a study in *Brassica napus* (Chen *et al.*, 2018). The reason might be that these novel miRNAs are species specific, and undetectable due to their low abundance.

MiRNA targets were mainly focused on upstream regulators, such as transcription factors (TFs) (Xie *et al.*, 2015). MiR396 regulates growth by targeting the GRFs and interacting with GIFs, in fact, miR396–GRF/GIF module responds to endogenous and environmental signals (Liebsch & Palatnik, 2020). MiR167 can target *ARF6* and *ARF8*, which are related to the auxin signaling pathway to induce cell wall loosening and expansion (Wu *et al.*, 2006; Perrot-Rechenmann, 2010; Zheng *et al.*, 2019). According to previous studies, ARF and Aux/IAA family members can directly up-regulate the expression of many GA genes, such as *GA20ox* and *GA2ox* during organ elongation (Y. Wang *et al.*, 2017). ARFs that regulated cell growth and development were significantly down-regulated in the internode at the bamboo growth decreasing stage (Wei *et al.*, 2018). During stamen development, GA regulates JA (Jasmonate) through DELLA, whereas *IAA8* directly or indirectly down-regulates JA through *ARF6* and *ARF8* (Huang *et al.*, 2017).

Most GRFs, which are upstream repressors of *KNOX* genes, can positively regulate cell proliferation in leaves and are more highly expressed in tender tissues than in mature tissues (Knaap *et al.*, 2000). *GRF*s targeted by miR396 in plants have various functions including GAs and CK biosynthesis, cell-wall modifications, plant development and disease resistance such as rice blast (Liu *et al.*, 2014; Omidbakhshfard *et al.*, 2015; Chandran *et al.*, 2019). *OsGRF1* is reported to induce GA biosynthesis in intercalary meristem (Knaap *et al.*, 2000). *AtGRF1* positively affect cell expansion (Kim *et al.*, 2003). *AtGRF4*, similar to *AtGRF1*, is also involved in cell proliferation (Omidbakhshfard *et al.*, 2015). *AtGRF5* and *BrGRF8* positively control cell proliferation during leaf development and overexpression of *AtGRF7* results in dwarf plants (Horiguchi *et al.*, 2005; Omidbakhshfard *et al.*, 2015). Overexpression of *ZmGRF10* in maize induces dwarfism by controlling cell proliferation. Similar to *ZmGRF10*, *AtGRF9* can also negatively regulate organ size (Wu *et al.*, 2014).

Similar to *ARF6*, *ARF8* expression gradually decreased from F4 to F1 and auxin content also reduced. The cell wall loosening and expansion ability of *ARF6* and *ARF8* became weaker, thus cells in F1 were obviously longer than F4 (Fig. 1). Higher *GRF1*, *ARF6*, and *ARF8* expression may induce GAs biosynthesis and cell division and growth in F4. All eleven *GRF*s related to cell proliferation had higher expression levels in F4 than in F1 (Fig. 4). Cell proliferation was vigorous in F4 but this ability reduced in F1. Some *GRF*s, such as *GRF6*, *7*, *9*, and *10*, had to be downregulated in order to avoid culm dwarfing.

Regulatory networks of DEMs, targets, hormones, and cells in the bamboo internode

Changes in upstream genes may have a significant impact on downstream genes in a signaling pathway. Most miRNAs are involved in complex networks and regulate various development processes (Tang & Chu, 2017). MiRNAs act on upstream regulators, and target to TFs (*GRF*s, *ARF*s, and *NAC*) and other genes. These genes may be linked to other related functional genes that affect cell growth and plant development, such as hormone signaling, DNA repair, and lignin biosynthesis.

Some miRNAs can target multiple gene families, such as miR396 targeting to *RECA*, *GRF*s, cyclin, cell wall related genes and miR164 targeting to *RECA*, *ANT* and *NAC* gene families, implying that target genes might change over time, between tissues or between species.

Cell cycle is driven by the complexes of cyclin and CDK (Inagaki & Umeda, 2011). MiR396 highly expressed in F1 causing reduction of GRF expression and delayed the cell cycle (Ercoli *et al.*, 2016), which proved that the cell division in F1 was weaker than in F4. In lignin biosynthesis, monolignols are polymerized into lignin through LAC (Laccase) in the cell wall (Berthet *et al.*, 2011; Yu *et al.*, 2020), and miR397 targeted to *LAC* genes. In this network, the expression level of miR397 in F1 was lower than that in F4 opposite to *LAC* expression, which was consistent with the fact that the upper part was more mature than the lower part of the internode.

Although some novel miRNAs were detected, further functional verification is still needed. Due to complicated transformation system in moso Bamboo, rice might be a good candidate system, but

there are still some gaps due to we did not find the perfect target genes of those bamboo novel miRNAs in rice, so there is still a long way to verify novel miRNA functions in bamboo.

Conclusion

In this study, the transcriptome, miRNAs and degradomes were investigated to learn more about bamboo rapid growth. The internode bottom cells mainly undergo cell division, while the upper section cells mainly undergo cell elongation and cell wall thickness till maturity. In bottom section miRNAs inhibited or degraded their targeted genes including TFs and other auxin, CKs and GAs genes mainly related to cell proliferation and cell division. In upper segments, miRNAs target genes including *NAC* TFs, the ABA pathway which are mainly involved in cell elongation and cell wall thickness.

Acknowledgement

This work was supported by the National Natural Science Foundation of China (31870653, 31670670, and 31811530009). The authors declare that they have no conflict of interest.

Contributions

K-lW, A-MW conceived the project and designed the experiments. K-lW and YZ performed the experiments. LS, H-MZ, X-CL and RX assisted in the research. K-lW and A-MW analyzed data and wrote the article. All the authors read and approved the final manuscript.

References

Addo-Quaye C, Eshoo TW, Bartel DP, Axtell MJ. 2008. Endogenous siRNA and miRNA targets identified by sequencing of the *Arabidopsis* degradome. *Current Biology* **18**(10): 758-762.

Berthet S, Demont-Caulet N, Pollet B, Bidzinski P, Cezard L, Le Bris P, Borrega N, Herve J, Blondet E, Balzergue S, et al. 2011. Disruption of *LACCASE4* and *17* results in tissue-specific alterations to lignification of *Arabidopsis thaliana* stems. *Plant Cell* **23**(3): 1124-1137.

Brown DM, Zeef LAH, Ellis J, Goodacre R, Turner SR. 2005. Identification of novel genes in *Arabidopsis* involved in secondary cell wall formation using expression profiling and reverse genetics. *Plant Cell* **17**: 2281-2295.

Bundy MG, Thompson OA, Sieger MT, Shpak ED. 2012. Patterns of cell division, cell differentiation and cell elongation in epidermis and cortex of *Arabidopsis* pedicels in the wild type and in erecta. *PLoS One* **7**(9): e46262.

Chandran V, Wang H, Gao F, Cao XL, Chen YP, Li GB, Zhu Y, Yang XM, Zhang LL, Zhao ZX, et al. 2019. miR396-*OsGRF*s module balances growth and rice blast disease-resistance. *Front Plant Science* **24**(9): 1999.

Chen L, Chen L, Zhang X, Liu T, Niu S, Wen J, Yi B, Ma C, Tu J, Fu T, et al. 2018. Identification of miRNAs that regulate silique development in *Brassica napus*. *Plant Science* **269**: 106-117.

Chen ML, Fu XM, Liu JQ, Ye TT, Hou SY, Huang YQ, Yuan BF, Wu Y, Feng YQ. 2012. Highly sensitive and quantitative profiling of acidic phytohormones using derivatization approach coupled with nano-LC-ESI-Q-TOF-MS analysis. *Journal of Chromatography B* **905**: 67-74.

Claeys H, De Bodt S, Inze D. 2014. Gibberellins and DELLAs: central nodes in growth regulatory networks. *Trends Plant Science* **19**(4): 231-239.

Cortleven A, Leuendorf JE, Frank M, Pezzetta D, Bolt S, Schmulling T. 2019. Cytokinin action in response to abiotic and biotic stresses in plants. *Plant Cell Environment* **42**(3): 998-1018.

Cosgrove DJ. 2015. Plant expansins: diversity and interactions with plant cell walls. *Current Opinion in Plant Biology* **25**: 162-172.

Daviere JM, Achard P. 2013. Gibberellin signaling in plants. *Development* **140**(6): 1147-1151.

Davies PJ 2010. The Plant Hormones: Their Nature, Occurrence, and Functions. In: Davies PJ ed. *Plant Hormones: Biosynthesis, Signal Transduction, Action!* Dordrecht: Springer Netherlands, 1-15.

Earley KW, Haag JR, Pontes O, Opper K, Juehne T, Song K, Pikaard CS. 2006. Gateway-compatible vectors for plant functional genomics and proteomics. *Plant Journal* **45**, 616-629

Ercoli MF, Rojas AM, Debernardi JM, Palatnik JF, Rodriguez RE. 2016. Control of cell proliferation and elongation by miR396. *Plant Signaling & Behavior* **11**(6): e1184809.

Eriksson S, Bohlenius H, Moritz T, Nilsson O. 2006. GA4 is the active gibberellin in the regulation of LEAFY transcription and *Arabidopsis* floral initiation. *Plant Cell* **18**(9): 2172-2181.

Fan C, Ma J, Guo Q, Li X, Wang H, Lu M. 2013. Selection of reference genes for quantitative real-time PCR in bamboo (*Phyllostachys edulis*). *PLoS One* **8**(2): e56573.

Fan XK, Tang S, Zhi H, He MM, Ma WS, Jia YC, Zhao BH, Jia GQ, Diao XM. 2017. Identification and fine mapping of *SiDWARF3* (*D3*), a pleiotropic locus controlling environment-independent dwarfism in foxtail millet. *Crop Science* **57**(5): 2431-2442.

Gamuyao R, Nagai K, Ayano M, Mori Y, Minami A, Kojima M, Suzuki T, Sakakibara H, Higashiyama T, Ashikari M, et al. 2017. Hormone distribution and transcriptome profiles in bamboo shoots provide insights on bamboo stem emergence and growth. *Plant & Cell Physiology* **58**(4): 702-716.

Ge W, Zhang Y, Cheng Z, Hou D, Li X, Gao J. 2017. Main regulatory pathways, key genes and microRNAs involved in flower formation and development of moso bamboo (*Phyllostachys edulis*). *Plant Biotechnol Journal* **15**(1): 82-96.

German MA, Pillay M, Jeong DH, Hetawal A, Luo S, Janardhanan P, Kannan V, Rymarquis LA, Nobuta K, German R, *et al.* 2008. Global identification of microRNA-target RNA pairs by parallel analysis of RNA ends. *Nnature Biotechnology* **26**(8): 941-946.

Hake S, Smith HM, Holtan H, Magnani E, Mele G, Ramirez J. 2004. The role of knox genes in plant development. *Annual Review of Cell and Developmental Biology* **20**: 125-151.

He CY, Cui K, Zhang JG, Duan AG, Zeng YF. 2013. Next-generation sequencing-based mRNA and microRNA expression profiling analysis revealed pathways involved in the rapid growth of developing culms in moso bamboo. *BMC Plant Biology* **13**: 119.

Horiguchi G, Kim GT, Tsukaya H. 2005. The transcription factor AtGRF5 and the transcription coactivator AN3 regulate cell proliferation in leaf primordia of *Arabidopsis thaliana*. *Plant Journal* **43**(1): 68-78.

Huang H, Liu B, Liu L, Song S. 2017. Jasmonate action in plant growth and development. *Journal of Experimental Botany* **68**(6): 1349-1359.

Inagaki S, Umeda M. 2011. Cell-cycle control and plant development. *International Review of Cell and Molecular Biology* **291**: 227-261.

Irshad M, Canut H, Borderies G, Pont-Lezica R, Jamet E. 2008. A new picture of cell wall protein dynamics in elongating cells of *Arabidopsis thaliana*: confirmed actors and newcomers. *BMC Plant Biology* **8**: 94.

Jaworek P, Kopecny D, Zalabak D, Sebela M, Kouril S, Hluska T, Koncitikova R, Podlesakova K, Tarkowski P. 2019. Occurrence and biosynthesis of cytokinins in poplar. *Planta* **250**(1): 229-244.

Jin QY, Peng HZ, Lin EP, Li N, Huang DN, Xu YL, Hua XQ, Wang KH, Zhu TJ. 2016. Identification and characterization of differentially expressed miRNAs between bamboo shoot and rhizome shoot. *Journal of Plant Biology* **59**(4): 322-335.

Kim JH, Choi D, Kende H. 2003. The AtGRF family of putative transcription factors is involved in leaf and cotyledon growth in *Arabidopsis*. *Plant Journal* **36**(1): 94-104.

Knaap Evd, Kim JH, Kende H. 2000. A novel gibberellin-induced gene from rice and its potential regulatory role in stem growth. *Plant Physiology* **122**: 695–704.

Korasick DA, Enders TA, Strader LC. 2013. Auxin biosynthesis and storage forms. *Journal of Experimental Botany* **64**(9): 2541-2555.

Kuang L, Shen Q, Wu L, Yu J, Fu L, Wu D, Zhang G. 2019. Identification of microRNAs responding to salt stress in barley by high-throughput sequencing and degradome analysis. *Environmental and Experimental Botany* **160**: 59-70.

Kumar M, Campbell L, Turner S. 2016. Secondary cell walls: biosynthesis and manipulation. *Journal of Experimental Botany* **67**(2): 515-531.

Kurihara Y, Watanabe Y. 2004. *Arabidopsis* micro-RNA biogenesis through Dicer-like 1 protein functions. *Proceedings of the National Academy of Sciences* **101**(34): 12753–12758.

Li L, Hu T, Li X, Mu S, Cheng Z, Ge W, Gao J. 2016. Genome-wide analysis of shoot growth-associated alternative splicing in moso bamboo. *Molecular Genetics and Genomics* **291**(4): 1695-1714.

Liebsch D, Palatnik JF. 2020. MicroRNA miR396, GRF transcription factors and GIF co-regulators: a conserved plant growth regulatory module with potential for breeding and biotechnology. *Current Opinion in Plant Biology* **53**: 31-42.

Liu J, Rice JH, Chen N, Baum TJ, Hewezi T. 2014. Synchronization of developmental processes and defense signaling by growth regulating transcription factors. *PLoS One* **9**(5): e98477.

Liu W, Xu ZH, Luo D, Xue HW. 2003. Roles of OsCKI1, a rice casein kinase I, in root development and plant hormone sensitivity. *Plant journal* **36**(2): 189-202.

Liu Z, Wei F, Feng Y-Q. 2010. Determination of cytokinins in plant samples by polymer monolith microextraction coupled with hydrophilic interaction chromatography-tandem mass spectrometry. *Analytical Methods* **2**(11): 1676.

Loix C, Huybrechts M, Vangronsveld J, Gielen M, Keunen E, Cuypers A. 2017. Reciprocal interactions between cadmium-induced cell wall responses and oxidative stress in plants. *Frontiers in Plant Science* **8**: 1867.

Long JM, Liu Z, Wu XM, Fang YN, Jia HH, Xie ZZ, Deng XX, Guo WW. 2016. Genome-scale mRNA and small RNA transcriptomic insights into initiation of citrus apomixis. *Journal of Experimental Botany* **67**(19): 5743-5756.

Mecchia MA, Debernardi JM, Rodriguez RE, Schommer C, Palatnik JF. 2013. MicroRNA miR396 and *RDR6* synergistically regulate leaf development. *Mechanisms of Development* **130**(1): 2-13.

Muro-Villanueva F, Mao X, Chapple C. 2019. Linking phenylpropanoid metabolism, lignin deposition, and plant growth inhibition. *Current Opinion in Biotechnology* **56**: 202-208.

Nanda AK, Melnyk CW. 2018. The role of plant hormones during grafting. *Journal of Plant Research* **131**(1): 49-58.

Olds CL, Glennon EKK, Luckhart S. 2018. Abscisic acid: new perspectives on an ancient universal stress signaling molecule. *Microbes and Infection* **20**(9-10): 484-492.

Omidbakhshfard MA, Proost S, Fujikura U, Mueller-Roeber B. 2015. Growth-Regulating Factors (GRFs): A small transcription factor family with important functions in plant biology. *Molecular Plant* **8**(7): 998-1010.

Peng Z, Lu T, Li L, Liu X, Gao Z, Hu T, Yang X, Feng Q, Guan J, Weng Q, et al. 2010. Genome-wide characterization of the biggest grass, bamboo, based on 10,608 putative full-length cDNA sequences. *BMC Plant Biology* **10**: 116.

Peng Z, Lu Y, Li L, Zhao Q, Feng Q, Gao Z, Lu H, Hu T, Yao N, Liu K, et al. 2013a. The draft genome of the fast-growing non-timber forest species moso bamboo (*Phyllostachys heterocycla*). *Nature Genetics* **45**(4): 456-461.

Peng Z, Zhang C, Zhang Y, Hu T, Mu S, Li X, Gao J. 2013b. Transcriptome sequencing and analysis of the fast growing shoots of moso bamboo (*Phyllostachys edulis*). *PLoS One* **8**(11): e78944.

Perrot-Rechenmann C. 2010. Cellular responses to auxin: division versus expansion. *C Cold Spring Harbor Perspectives in Biology* **2**(5): a001446.

Rogers LA, Campbell MM. 2004. The genetic control of lignin deposition during plant growth and development. *New Phytologist* **164**(1): 17-30.

Rooij E, Olson EN. 2007. MicroRNAs: powerful new regulators of heart disease and provocative therapeutic targets. *The Journal of Clinical Investigation* **117**(9): 2369-2376.

Schaller GE, Bishopp A, Kieber JJ. 2015. The yin-yang of hormones: cytokinin and auxin interactions in plant development. *Plant Cell* **27**(1): 44-63.

Shan X, Yang K, Xu X, Zhu C, Gao Z. 2019. Genome-wide investigation of the nac gene family and its potential association with the secondary cell wall in moso bamboo. *Biomolecules* **9**(10): 609. doi: 10.3390/biom9100609.

Suzuki K, Itoh T. 2001. The changes in cell wall architecture during lignification of bamboo, *Phyllostachys aurea* Carr. *Trees* 15(3): 137-147.

Shinozaki K, Yamaguchi-Shinozaki K. 2006. Gene networks involved in drought stress response and tolerance. *Journal of Experimental Botany* **58**(2): 221-227.

Takatsuka H, Umeda M. 2019. ABA inhibits root cell elongation through repressing the cytokinin signaling. *Plant Signaling & Behavior* **14**(3): e1578632.

Tameshige T, Hirakawa Y, Torii KU, Uchida N. 2015. Cell walls as a stage for intercellular communication regulating shoot meristem development. *Frontiers in Plant Science* **6**: 324.

Tang J, Chu C. 2017. MicroRNAs in crop improvement: fine-tuners for complex traits. *Nature Plants* **3**: 17077.

Tao GY, Ramakrishnan M, Vinod KK, Yrjala K, Satheesh V, Cho J, Fu Y, Zhou M. 2020. Multi-omics analysis of cellular pathways involved in different rapid growth stages of moso bamboo. *Tree Physiology* **40**(11): 1487-1508.

Tsuyama T, Shimada N, Motoda T, Matsushita Y, Kijidani Y, Fukushima K, Kamei I. 2017. Lignification in developing culms of bamboo *Sinobambusa tootsik*. *Journal of Wood Science* **63**(6): 551-559.

Vanholme R, De Meester B, Ralph J, Boerjan W. 2019. Lignin biosynthesis and its integration into metabolism. *C Current Opinion in Biotechnology* **56**: 230-239.

Wang CY, Zhang S, Yu Y, Luo YC, Liu Q, Ju C, Zhang YC, Qu LH, Lucas WJ, Wang X, et al. 2014. MiR397b regulates both lignin content and seed number in *Arabidopsis* via modulating a laccase involved in lignin biosynthesis. *Plant Biotechnol Journal* **12**(8): 1132-1142.

Wang H, Zhao Q, Chen F, Wang M, Dixon RA. 2011. NAC domain function and transcriptional control of a secondary cell wall master switch. *Plant Journal* **68**(6): 1104-1114.

Wang HY, Cui K, He CY, Zeng YF, Liao SX, Zhang JG. 2015. Endogenous hormonal equilibrium linked to bamboo culm development. *Genetics and Molecular Research* **14**(3): 11312-11323.

Wang KL, Wang B, Hu R, Zhao X, Li H, Zhou G, Song L, Wu AM. 2019. Characterization of hemicelluloses in Phyllostachys edulis (moso bamboo) culm during xylogenesis. *Carbohydrate Polymers* **221**: 127-136.

Wang W, Gu L, Ye S, Zhang H, Cai C, Xiang M, Gao Y, Wang Q, Lin C, Zhu Q. 2017. Genome-wide analysis and transcriptomic profiling of the auxin biosynthesis, transport and signaling family genes in moso bamboo (*Phyllostachys heterocycla*). *BMC Genomics* **18**(1): 870.

Wang Y, Chantreau M, Sibout R, Hawkins S. 2013. Plant cell wall lignification and monolignol metabolism. *Frontiers in Plant Science* **4**: 220.

Wang Y, Zhao J, Lu W, Deng D. 2017. Gibberellin in plant height control: old player, new story. *Plant Cell Reports* **36**(3): 391-398.

Wei Q, Guo L, Jiao C, Fei Z, Chen M, Cao J, Ding Y, Yuan Q. 2019. Characterization of the developmental dynamics of the elongation of a bamboo internode during the fast growth stage. *Tree Physiology* **39**(7): 1201-1214.

Wei Q, Jiao C, Ding Y, Gao S, Guo L, Chen M, Hu P, Xia S, Ren G, Fei Z. 2018. Cellular and molecular characterizations of a slow-growth variant provide insights into the fast growth of bamboo. *Tree Physiology* **38**(4): 641-654.

Weiss D, Ori N. 2007. Mechanisms of cross talk between gibberellin and other hormones. *Plant Physiology* **144**(3): 1240-1246.

Wen X, Sun L, Chen Y, Xue P, Yang Q, Wang B, Yu N, Cao Y, Zhang Y, Gong K, et al. 2020. Rice dwarf and low tillering 10 (*OsDLT10*) regulates tiller number by monitoring auxin homeostasis. *Plant Science* **297**: 110502.

Wu L, Zhang D, Xue M, Qian J, He Y, Wang S. 2014. Overexpression of the maize *GRF10*, an endogenous truncated growth-regulating factor protein, leads to reduction in leaf size and plant height. *Journal of Integrative Plant Biology* **56**(11): 1053-1063.

Wu MF, Tian Q, Reed JW. 2006. *Arabidopsis microRNA167* controls patterns of *ARF6* and *ARF8* expression, and regulates both female and male reproduction. *Development* **133**(21): 4211-4218.

Xie F, Jones DC, Wang Q, Sun R, Zhang B. 2015. Small RNA sequencing identifies miRNA roles in ovule and fibre development. *Plant Biotechnology Journal* **13**(3): 355-369.

Yamaguchi S. 2008. Gibberellin metabolism and its regulation. *Annual Review of Plant Biology* **59**: 225–251.

Yoon J, Choi H, An G. 2015. Roles of lignin biosynthesis and regulatory genes in plant development. *Journal of Integrative Plant Biology* **57**(11): 902-912.

Yu X, Gong H, Cao L, Hou Y, Qu S. 2020. MicroRNA397b negatively regulates resistance of *Malus hupehensis* to *Botryosphaeria dothidea* by modulating *MhLAC7* involved in lignin biosynthesis. *Plant Science* **292**: 110390.

Zhang H, Wang H, Zhu Q, Gao Y, Wang H, Zhao L, Wang Y, Xi F, Wang W, Yang Y, et al. 2018. Transcriptome characterization of moso bamboo (*Phyllostachys edulis*) seedlings in response to exogenous gibberellin applications. *BMC Plant Biology* **18**(1): 125.

Zhao H, Wang L, Dong L, Sun H, Gao Z. 2014. Discovery and comparative profiling of microRNAs in representative monopodial bamboo (*Phyllostachys edulis*) and sympodial bamboo (*Dendrocalamus latiflorus*). *PLoS One* **9**(7): e102375.

Zheng L, Nagpal P, Villarino G, Trinidad B, Bird L, Huang Y, Reed JW. 2019. miR167 limits anther growth to potentiate anther dehiscence. *Development* **146**(14): 174375. doi: 10.1242/dev.174375.

Zhou B, Fu M, Xie J, Yang X, Li Z. 2005. Ecological functions of bamboo forest: research and application. *Journal of Forestry Research* **16**(2): 143-147.

The following Supplementary Material is available for this article:

Fig. S1 The growth rate of moso bamboo culm internodes was calculated at next few time points.

Fig. S2 The schematic diagram of collected samples.

Fig. S3 Principal component analysis (PCA) of F1 - UF4 samples.

Fig. S4 Clusters of total genes and KEGG pathway annotations of profile 8, 9 and 18, respectively.

Fig. S5 Venn diagram of F1, F2, F3, and UF4 were compared with F4, respectively.

Fig. S6 KEGG pathway enrichment of DEGs that F1, F2, F3 and UF4 compared with F4, respectively.

Fig. S7 Expression pattern of six genes associated with cell division.

Fig. S8 MiRNA length distribution of known and novel miRNA.

Fig. S9 Total trends of different expression target genes of DEMs.

Fig. S10 KEGG pathway annotation of cluster 8, 9 and 18 of target genes, respectively.

Fig. S11 The miRNA cleavage sites of five validated target genes predicted by target plots (t-plots).

Table S1 Primers list for qPCR analysis of gene expression and vector construction.

Table S2 Summary of transcriptome mapping.

Table S3 Data of F1 and F4 degradome sequencing.

Table S4 Information of degraded genes in F1 and F4 degradomes.

Table S5 MiRNA and their target genes information for qPCR.

Table S6 RT and qPCR primers list of miRNAs.

Figure legends

Fig. 1. The samples of fast-growth potential bamboo internode and the cell appearances of longitudinal section were displayed in *Phyllostachys edulis* (moso bamboo). Bamboo culm showed the fast growth internode in natural state. The target internode was equally divided into four segments referred as F1-F4 and upper internode was regarded as UF4. a-d are longitudinal section of samples corresponding with F1-F4, respectively, and bar is 20 μm. Paraffin sections were under light microscope observed after stained in safranin O and fast green FCF solutions. Cell size getting bigger from F4 to F1. e-h are 2 μm ultra-thin cross section of F1-F4, bar is 1 μm. Red arrow labelled to cell wall. sections were observed under transmission electron microscope after staining the samples by 2.5% glutaraldehyde fixative solution. Cell wall getting more and more thickness from F4 - F1. i-l are cross sections of F4 at the different cell division stages, bar is 20 μm. i, prophase; j, metaphase; k, anaphase and l, telophase. Cell numbers (m) and cell length (n) were compared in four type longitudinal cross sections. Data is means ± SD. Random selected 5 views of four samples in longitudinal sections and counted the cell number then calculated the averaged and SD. Followed the same method to calculate the cell length. In general, cell number decreased from F4 to F1 but cell length was opposite.

Fig. 2 Important hormone contents were measured in F1 and F4. The hormone contents of F1 and F4 samples were detected by LC-MS. Value is means ± SD (Unit: ng/g F.W.). a-d are Gibberellin 1 (GA1), GA3, GA4 and GA7, respectively, due to only GA1, 3, 4 and 7 have biological activity. The contents of GA1, 3, 4 and 7 in F4 were higher than them in F1. e is indoleacetic acid (IAA). IAA is the best-studied naturally occurring and active auxin. The content of IAA in F4 was higher than that in F1. f is abscisic acid (ABA). The content of ABA in F4 was lower than that in F1. g and h are isopentenyladenine (iP) and trans-zeatin (tZ), respectively. Cis-zeatin (cZ) and dihydrozeatin (DZ) were not detected in F1 and F4. The contents of iP and tZ in F4 were higher than them in F1. i is GAs referring sum of GA1, 3, 4 and 7. j is Cytokinins (CKs) referring sum of iP and tZ. ** when $p < 0.01$, * when $p < 0.05$ based on ANOVA (Analysis of variance) method. The contents of GAs and CKs in F4 were higher than them in F1. In generally, the hormone level in F4 were higher than them in F1 except ABA.

Fig. 3 log_2FC of differentially expressed miRNAs (DEMs) in F1 VS F4 and KOG analysis of differentially expressed genes (DEGs) in four different patterns. a, 51 known DEMs when F1 was referenced to F4. b, 12 novel DEMs when F1 was referenced to F4. The *y*-axis indicates the value of log_2FC (FC, fold change). The *x*-axis is DEMs name. There are 63 DEMs (51 known and 12 novel miRNAs) when F1 was referenced to F4 and parameter were false discovery rate (FDR) ≤ 0.05 FC ≥ 1.5. The most abundant miRNA of 51 known DEMs was miR396, and the second was miR167, expression level of 12 novel DEMs generally were lower than known ones. c, there were 734 target DEGs of 63 DEMs when F1 was referenced to F4 and parameter was FDR ≤ 0.05 and $|log_2FC| \geq 1$. The *y*-axis of each cluster indicated the value of log_2FC. Clusters were obtained by STEM software using 734 DEGs expression profiles. The parameters are p - value ≤ 0.05 and minimum changed fold is 2. KOG analysis were applied to 4 clusters. The *y*-axis of the each KOG analysis is number of genes. The *y*-axis of each cluster indicates the value of log_2FC. KOG analysis was applied to 4 clusters. The *y*-axis of the each KOG analysis is number of genes. Cluster 8 was most abundant cluster with 304 DEGs. The gene expression trend was roughly decreased from F4 and F3 to F2 and F1 then rose again in UF4. The second abundant was cluster 9 with 112 genes which had roughly opposite gene expression trends with Cluster 8. The KOG of cluster 8 was mainly cell division genes, but the numbers of cell division gene in cluster 9 were decreased and more genes were related to other transport and metabolism process.

Fig. 4 Heatmap of 12 differentially expressed miRNAs (DEMs) and their 21 different expression target genes in F1 and F4 degradomes. a, heatmap of DEMs. The heatmap obtained by their log_2FC when F1 was referenced to F4. b, heatmap of 21 different expression target genes in F1 and F4 degradomes. The heatmap observed by TBtools based on their FPKM of RNA_seq. The right column were corresponding with gene IDs and gene names, respectively, and samples were labelled at the below of heatmap. The color bar is the scale for the expression levels of each gene. 21 genes can divide into two classes based on their gene expression pattern. Gene expression level of Class I in F1 were higher than them in F4 but gene expressions of Class II were opposite. And all genes in Class I are *ARF*s and *GRF*s.

Fig. 5 Gene verification of transcriptome and miRNA. a-l, qPCR analysis of 12 candidate genes expression pattern from F1 to F4 samples. The *y*-axis of each gene is the relative expression level value which obtained by referenced to *NTB*. The calculated method is $2^{-\Delta Ct}$. Bars represent mean values of three replicates ± SD. a, *CYCB1-5* (*PH02Gene02370*); b, *UBA1C* (*PH02Gene24566*); c, *CYCD2-1* (*PH02Gene27422*); d, *GUX2* (*PH02Gene10406*); e, *CCOAOMT2* (*PH02Gene12695*); f, *CESA8* (*PH02Gene45360*); g, *ARF12* (*PH02Gene43144*); h, *IQD32* (*PH02Gene46249*); i, *SETH3* (*PH02Gene40412*); j, *NMT1* (*PH02Gene21093*); k, *KIN-12A* (*PH02Gene23920*); l, *GRF6* (*PH02Gene26399*). a - c, are cell cycle genes; d - f, are secondary cell wall related genes; g and h are hormone related genes; i – l, are related to other process genes including lipid, microtubule, GRF and carbohydrate. a-c, their expression level decreased gradually from F4 to F1 and rise in UF4. d-f, their expression levels were increasing approximately from F4 to F1 and fall in UF4. g and i - l gene expression level is similar to a-c but h is similar to d-f. These genes expression trend is similar to RNA-Seq expression data. m-u, miRNA and their target genes expression pattern from F1 to F4 samples. The *y*-axis of each gene is the relative expression level value which referenced to *NTB* and F4. The calculated method is $2^{-\Delta\Delta Ct}$. Bars represent mean values of three replicates ± SD. m, *VIL2* (*PH02Gene39446*); n, *ARF8* (*PH02Gene37247*); o, *GRF1* (*PH02Gene 34199*); p, *GRF10* (*PH02Gene01484*); q, *GRF4* (*PH02Gene08777*); r, *KIN-12A* (*PH02Gene23920*); s, *CYCB1-5* (*PH02Gene43240*); t, *NAC035* (*PH02Gene07908*); u, *CSLC2* (*PH02Gene09964*). The expression level of PemiR164a-3, PemiR167d-4, PemiR396e-4 and PemiR396f-3 roughly increased from F4 to F1. The expression level of their target genes was roughly decreasing from F4 to F1. But expression levels of PemiR529d, PemiR529e-2 and their target genes showed the opposite way compared to m-s. MiRNAs and their target genes were complementary.

Fig. 6 Validation of miR_N17, miR_N31, miR396a-3, miR444b-1 and their target genes. a, EV (empty vector), miR-OE and target genes overexpression vectors constructed for transient expression in *Nicotiana benthamiana*. b, miRNAs and their target sites information. miR_N17, miR_N31, miR396a-3 and miR444b-1 can inhibited target genes' expression. c, control and co-infiltrated leaf under Nightshade LB985 after infiltration. The first tobacco leaf was under the

brightfield and next four pair miR-target leaves were under the GFP filter. The left/right pictures of one leaf were co-infiltrated with miR/EV and target gene fusing with GFP, respectively.

Fig. 7 The network of miRNA, targets, hormones and cell growths in bamboo internode rapid growth stage. Blue-black arrow, expression trend of miRNA which in F1 referenced to F4. Black arrow referring to promote or participate; black dotted blunt ended line referring to inhabit. The cell morphology of F4 - F1 and growth schematic diagram of internode bottom to up are under the network. Bar is 20 μm. 8 differentially expressed miRNAs (DEMs) expression levels in F1 are higher than that in F4, and 6 DEMs are opposite. While all 14 miRNAs are negatively regulated their target genes. All DEMs were FC ≥ 1.5, except miR397 and miR164a. So we labeled miR397 and miR164a with hollow circles and the rest DEMs labeled with solid brown circles, and all differentially expressed genes (DEGs), except *NAC* which targeted by miR164a , in this network were FC ≥ 2. So miR164a target *NAC* with blue line. Their targets are form a network connected to hormones and regulate cell growth processes. Cell size become bigger from F4 to F1 and cell wall also become thicker.

nph_17542_f1-8.pptx

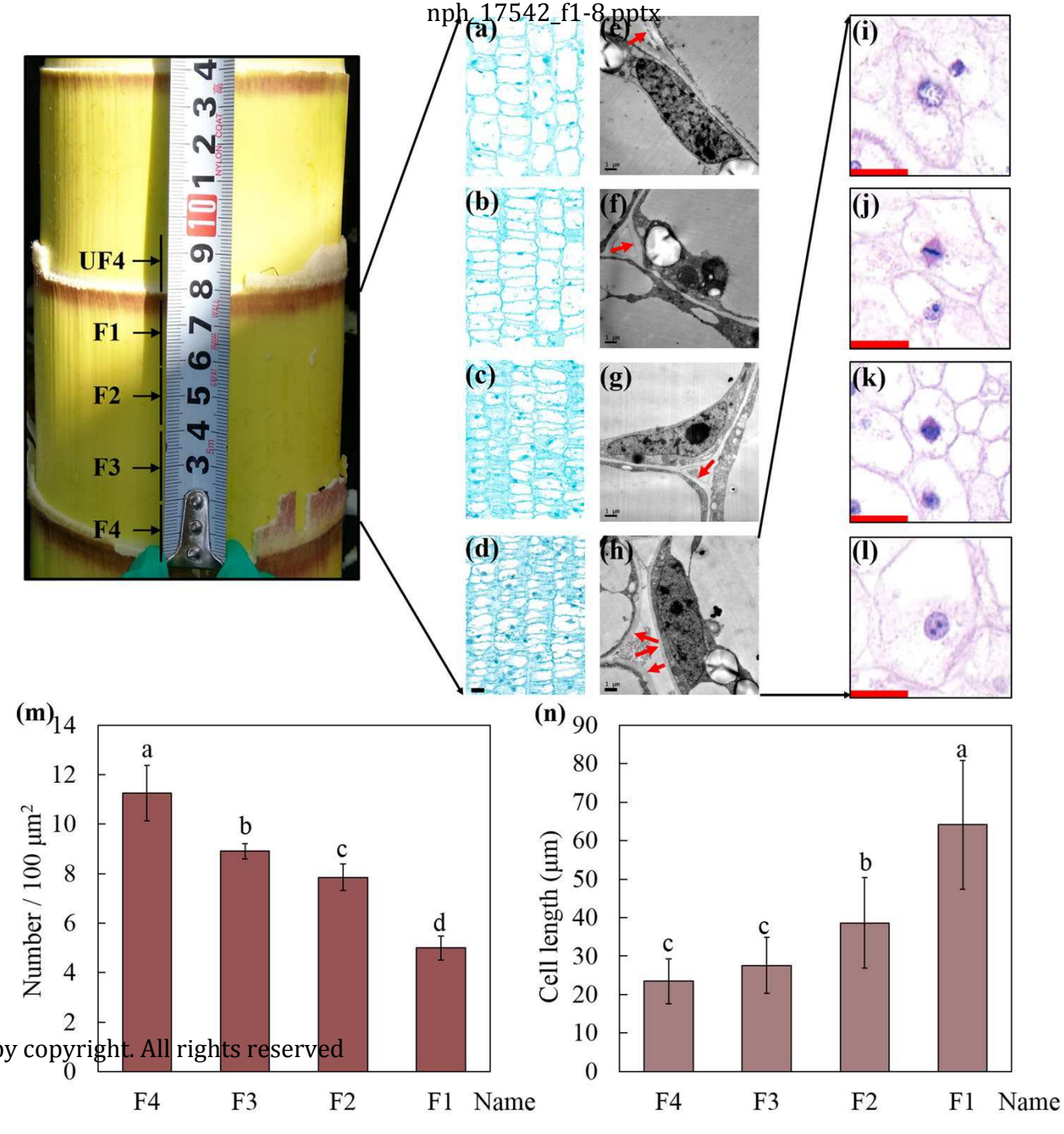

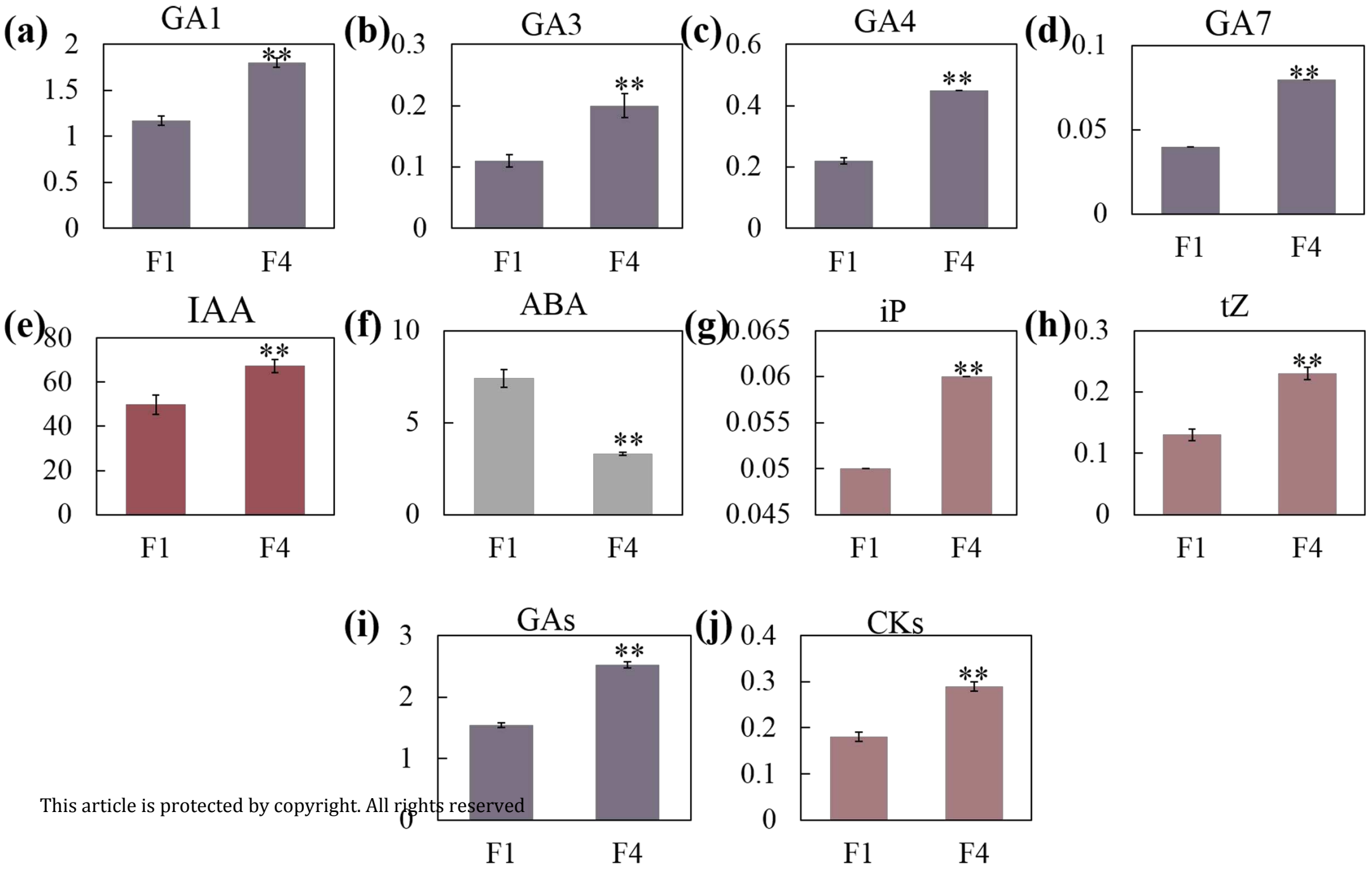

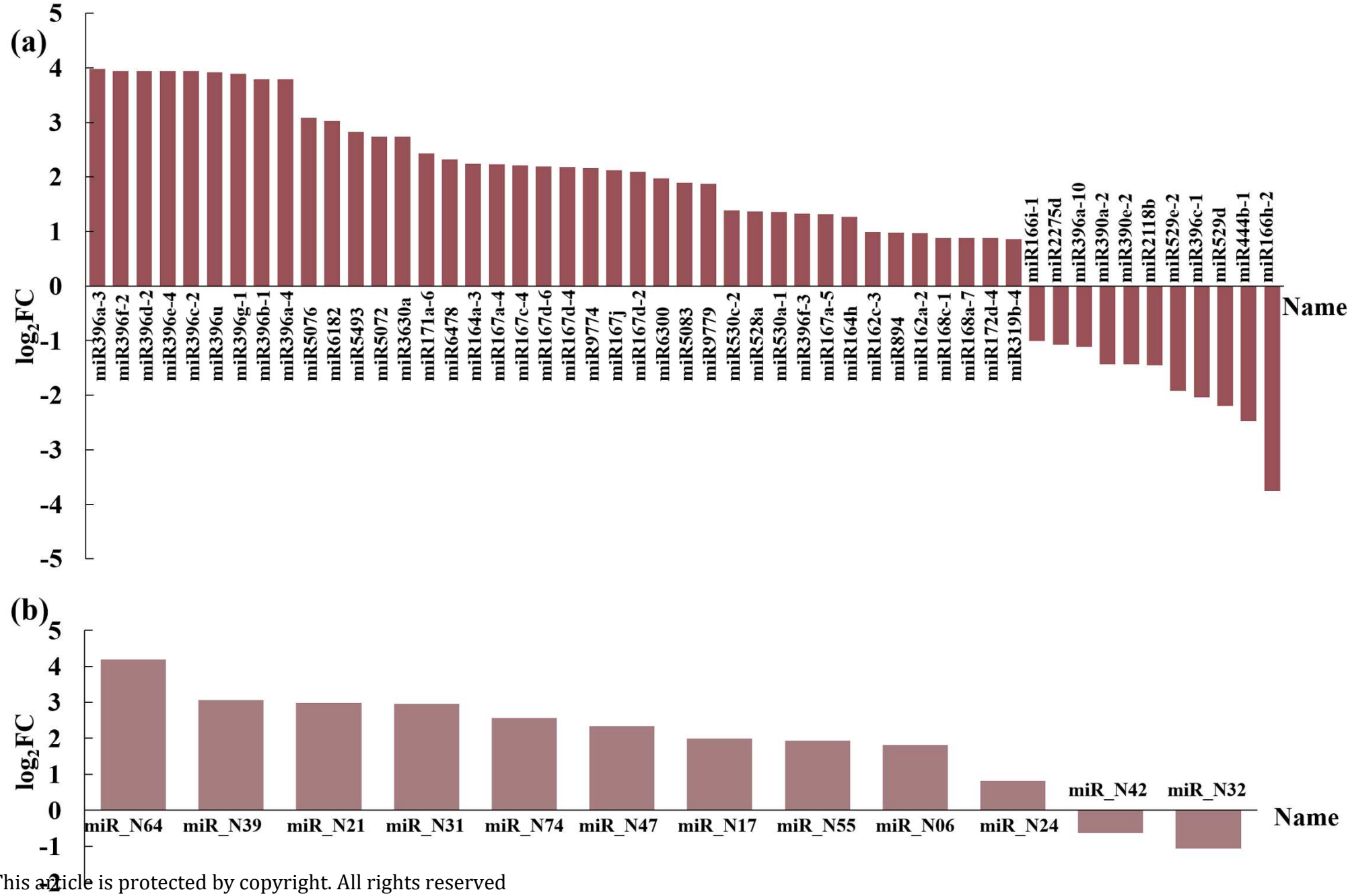

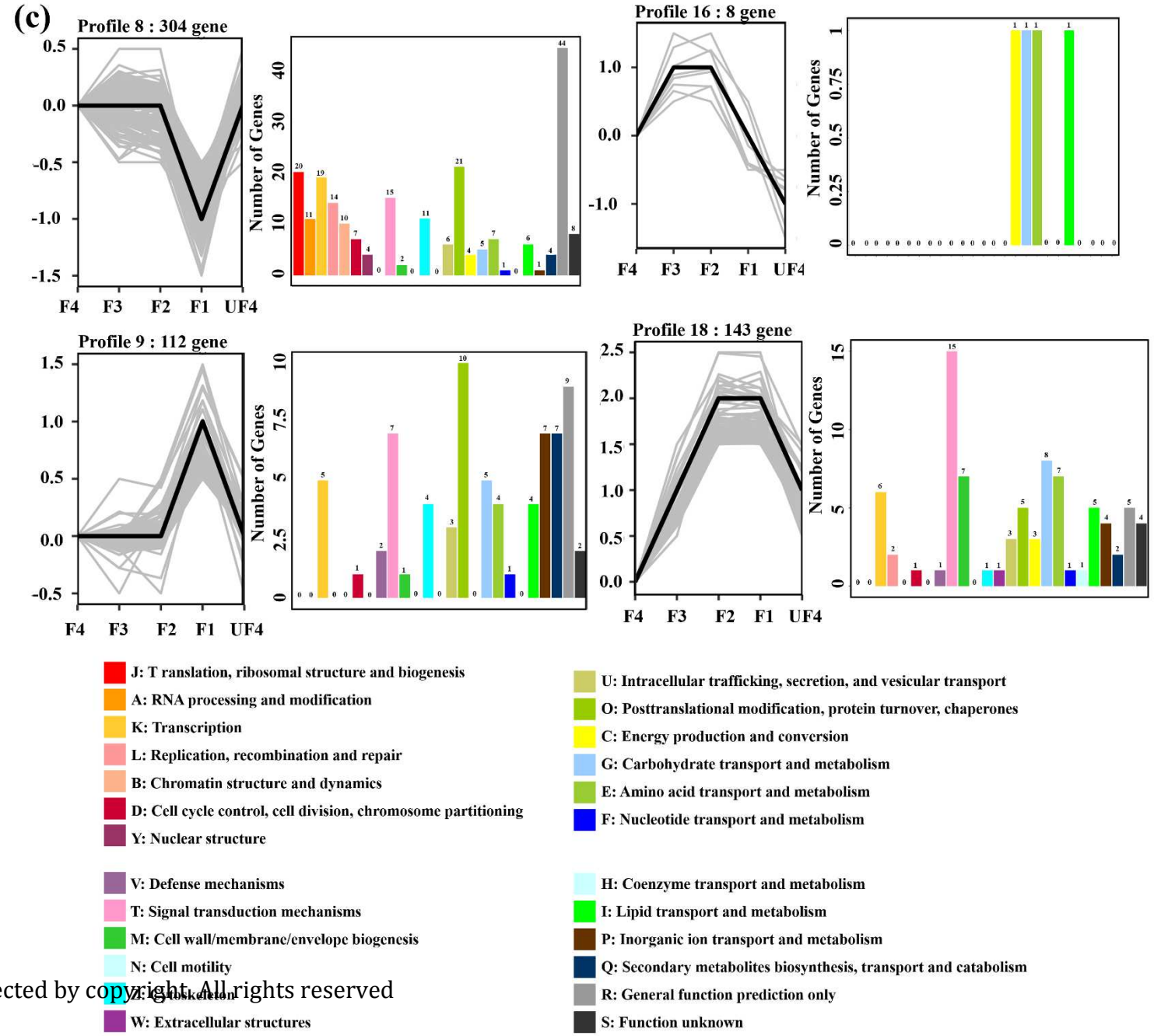

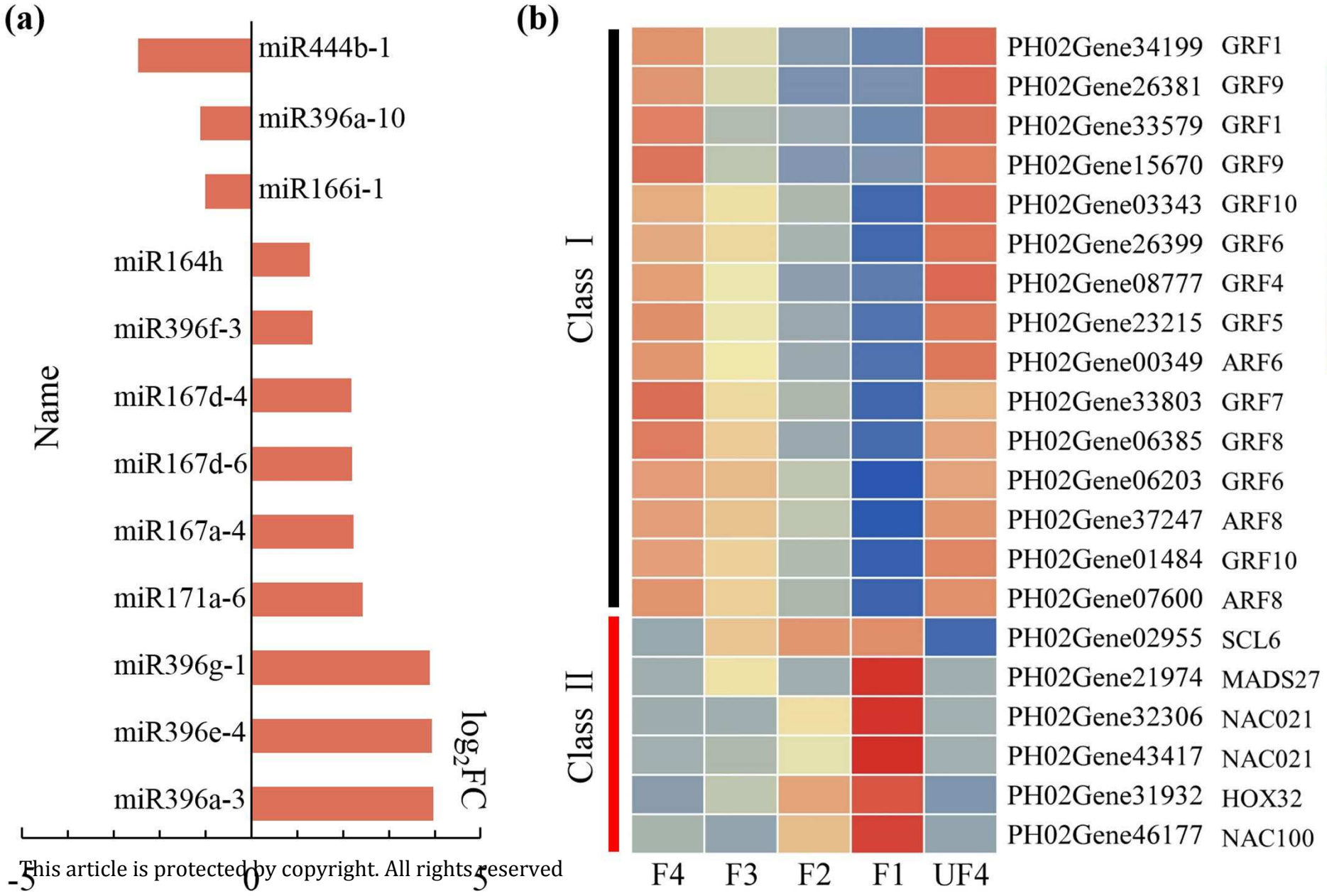

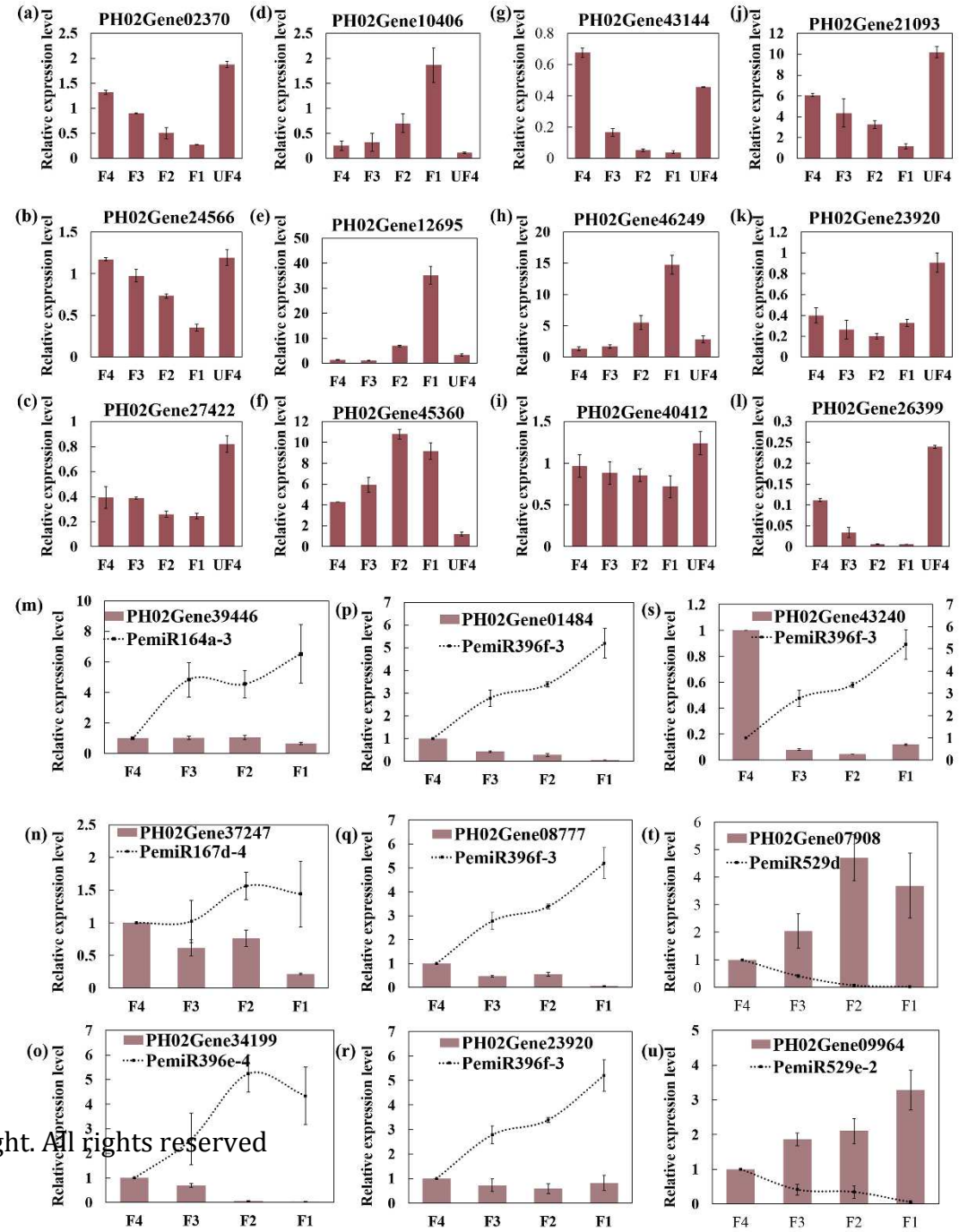

(a)

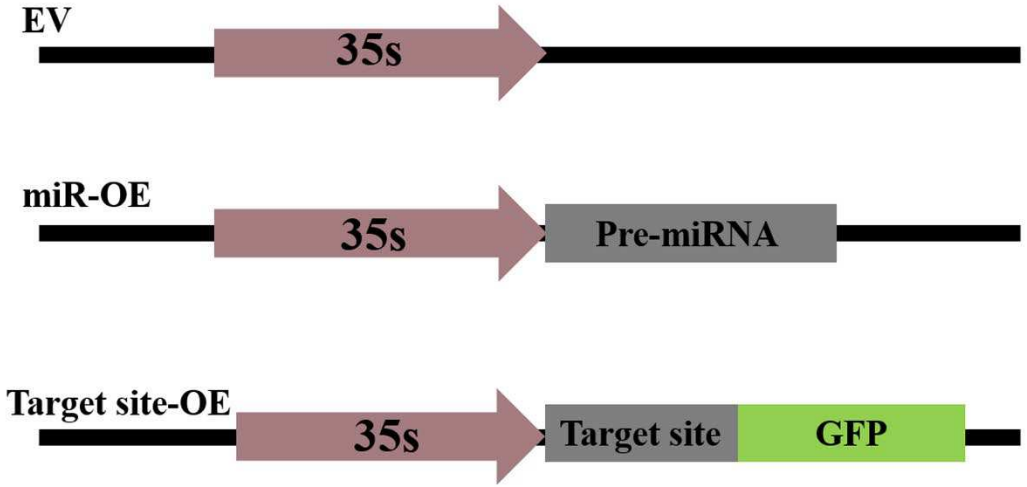

(b)

```
miR_N31          3' UUUGUAUCACGUUUCAGUUCU 5'
                    :|||||  ||  |||||:|   |||||
PH02Gene45537    5' GAACAU-GUGCAAGGGCAAGA 3'

miR_N17          3' UUA-AUAGCGUCUGCCAAGAACA 5'
                     |:|  |||:  |||||||||||||  |
PH02Gene29128    5' AGUCUAUUCCAGACGGUUCUUCU 3'

miR444b-1        3' UUCGAACUCUGUCGUUGACGU 5'
                    |||||||||||||   ||||||||
PH02Gene21974    5' AAGCUUGAGACAACAACUGCA 3'

miR396a-3        3' UACAAGUUCUUUCGGACACCU 5'
                    |||||||||||:|||||||
PH02Gene01484    5' CCGUUCAAGAAAGUCUGUGGA 3'
```

(c)